

# Chromatin Regulators as a Guide for Cancer Treatment Choice

Zachary A. Gurard-Levin<sup>1,2</sup>, Laurence O.W. Wilson<sup>1,2</sup>, Vera Pancaldi<sup>3</sup>, Sophie Postel-Vinay<sup>4,5,6</sup>, Fabricio G. Sousa<sup>7</sup>, Cecile Reyes<sup>8</sup>, Elisabetta Marangoni<sup>8</sup>, David Gentien<sup>8</sup>, Alfonso Valencia<sup>3</sup>, Yves Pommier<sup>7</sup>, Paul Cottu<sup>9</sup>, and Geneviève Almouzni<sup>1,2</sup>

## Abstract

The limited capacity to predict a patient's response to distinct chemotherapeutic agents is a major hurdle in cancer management. The efficiency of a large fraction of current cancer therapeutics (radio- and chemotherapies) is influenced by chromatin structure. Reciprocally, alterations in chromatin organization may affect resistance mechanisms. Here, we explore how the misexpression of chromatin regulators—factors involved in the establishment and maintenance of functional chromatin domains—can inform about the extent of docetaxel response. We exploit Affymetrix and NanoString gene expression data for a set of chromatin regulators generated from breast cancer patient-derived xenograft models and patient samples treated with doc-

etaxel. Random Forest classification reveals specific panels of chromatin regulators, including key components of the SWI/SNF chromatin remodeler, which readily distinguish docetaxel high-responders and poor-responders. Further exploration of SWI/SNF components in the comprehensive NCI-60 dataset reveals that the expression inversely correlates with docetaxel sensitivity. Finally, we show that loss of the SWI/SNF subunit BRG1 (SMARCA4) in a model cell line leads to enhanced docetaxel sensitivity. Altogether, our findings point toward chromatin regulators as biomarkers for drug response as well as therapeutic targets to sensitize patients toward docetaxel and combat drug resistance. *Mol Cancer Ther*; 15(7): 1768–77. ©2016 AACR.

## Introduction

Chromatin regulators—histone variants (1), histone chaperones (2), DNA and histone modifying enzymes, effector proteins, and chromatin remodelers (3)—cooperate to bridge chromatin organizational scales from nucleosome assembly to the establishment of functional chromatin domains. The centromere, for example, features a distinct histone variant, CenH3 (also called CENP-A; ref. 4), which marks the site of kinetochore assembly and microtubule attachment required for proper chromosome segregation (5). Notably, the aberrant expression or mutation of many chromatin regulators is linked to

various cancers (reviewed in ref. 6). Furthermore, overexpression of CenH3, a hallmark of aggressive cancers, enables a rewiring of interactions that alter chromatin organization and affect how cells respond to DNA damage inducing agents, highlighting the biologic consequences of dosage imbalances in chromatin regulators (7). Thus, understanding the misregulation of chromatin regulators in cancer will facilitate diagnostics and therapeutics.

The challenge of precision medicine is to identify the optimal anticancer treatment regimen for individual patients. Current treatments for breast cancer exploit pathologic and clinical parameters (age, tumor size, grade, and node status), as well as the classical biomarkers oestrogen receptor (ER), progesterone receptor (PR), HER2 (also known as ERBB2), and the proliferation status as assessed with the marker Ki67 (8). These readouts help place the patient into one of the four original molecular subtypes having various responses to therapy. More recently, gene expression profiling has enabled the development of commercial prognostic transcriptomic tests, such as MammaPrint, Oncotype DX, and Prosigna (PAM50), to help distinguish patients with high risk from low risk of recurrence and to aid treatment choices (9–11), ideally as a Go / No-Go decision for chemotherapy. However, these tests are restricted to ER-positive patients, and their predictive value might be limited (12, 13). As a consequence, only 2% to 15% of early-stage breast cancer patients will clinically benefit from the adjuvant chemotherapy they receive (14). This dramatically low rate is likely due to a combination of chemotherapy overtreatment (overestimation of poor prognosis) and mistreatment (lack of predictive information).

Emerging data demonstrate that the misregulation of chromatin regulators contributes to tumorigenesis (6), tumor

<sup>1</sup>Institut Curie, PSL Research University, CNRS, UMR3664, Equipe Labellisée Ligue contre le Cancer, Paris, France. <sup>2</sup>Sorbonne Universités, UPMC Université Paris 06, CNRS, UMR3664, Paris, France. <sup>3</sup>Spanish National Cancer Research Centre (CNIO), c/Melchor Fernández, Almagro, Madrid, Spain. <sup>4</sup>DITEP (Département d'Innovations Thérapeutiques et Essais Précoces), Gustave Roussy, France. <sup>5</sup>Inserm Unit U981, Gustave Roussy, Villejuif, France. <sup>6</sup>Université Paris Saclay, Université Paris-Sud, Faculté de Médecine, Le Kremlin Bicêtre, France. <sup>7</sup>Developmental Therapeutics Branch and Laboratory of Molecular Pharmacology, Center for Cancer Research, National Cancer Institute, NIH, Bethesda, Maryland. <sup>8</sup>Institut Curie, PSL Research University, Translational Research Department, Genomics Platform, Paris, France. <sup>9</sup>Institut Curie, Medical Oncology, Paris, France.

**Note:** Supplementary data for this article are available at Molecular Cancer Therapeutics Online (<http://mct.aacrjournals.org/>).

**Corresponding Authors:** Zachary A. Gurard-Levin, Institut Curie, 26 rue d'Ulm, Paris 75005, France. Phone: 33156246702; Fax: 33146333016; E-mail: zachary.gurard-levin@curie.fr; and Geneviève Almouzni, genevieve.almouzni@curie.fr

**doi:** 10.1158/1535-7163.MCT-15-1008

©2016 American Association for Cancer Research.

heterogeneity (15), and the cellular response to anticancer drugs (7, 16–19). It offers the hope to exploit chromatin factors to guide treatment decisions. Indeed, radiotherapy and many standard-of-care chemotherapies act by directly binding or damaging DNA (e.g., anthracyclines, topoisomerase inhibitors, crosslinking agents) or during processes that rely on chromatin architecture (e.g., taxanes). Docetaxel, a member of the taxane family, binds microtubules and prevents their depolymerization and thereby cell division (20). Docetaxel is one of the most active anticancer agents, used in breast, lung, prostate, stomach, and head/neck cancers, yet less than half of the patients respond and resistance is a major challenge. Notably, there is no clinically available predictive marker for docetaxel efficacy (21, 22). Given that microtubules attach at kinetochores assembled at centromeres, we hypothesize that the misregulation of the expression or function of chromatin regulators may affect the make-up of the chromosome and in turn affect docetaxel efficacy. Prompted by studies linking taxane response to the expression of two chromatin regulators—the histone deacetylase HDAC7 (23) and the histone chaperone DAXX (24)—we performed a global unbiased analysis of chromatin regulator gene expression in docetaxel high-responders and poor-responders and examined how they may vary in distinct settings.

Although there are several advantages in exploiting cell lines in drug response studies, including their adaptability to high-throughput approaches and cost-effective genetic tools to generate hypotheses, several drawbacks limit the translation to *in vivo* models, such as a homogenous population and a small therapeutic window. Here, we use data from several preclinical model systems and analyze the expression of chromatin regulators in samples displaying a broad range of responses to docetaxel. Starting with available gene expression data from Affymetrix microarrays, we could correlate the expression of a panel of chromatin regulators selectively to the docetaxel response in a cohort of breast cancer patient-derived xenograft (PDX) models (25, 26). We also observe a similar correlation in organoids derived from colorectal cancer patients (27). We further exploit the quantitative NanoString technology (28) to measure gene expression for chromatin regulators in the tumors of patients treated at the Institut Curie. Based on these analyses, we describe a panel of chromatin regulators that can robustly segregate patient high-responders and poor-responders. Notably, we identify the SWI/SNF chromatin remodeler as a novel factor associated with the docetaxel response. Our data point to the benefit of including chromatin regulators in the clinic to validate their potential as markers of the docetaxel response and extend this approach to other drugs. We describe a new mechanism to sensitize tumors to docetaxel by targeting the SWI/SNF complex and potentially combat inherent and acquired resistance.

## Materials and Methods

### Selection of chromatin regulators and NanoString nCounter codeset

We selected 551 genes coding for histone variants, histone chaperones, chromatin remodelers, DNA and histone modifying enzymes, effector proteins that recognize and bind chromatin, and any gene having a Gene Ontology term related to chromatin binding or chromatin regulation (Supplementary Fig. S1). We focused on these genes in our analysis of available

Affymetrix gene expression data for the patient-derived xenograft models. For the 9 PDX models and the Institut Curie patient cohort, we ordered a custom NanoString codeset for the 551 chromatin regulators as well as housekeeping genes and genes implicated in breast cancer such as oestrogen receptor (ESR1), progesterone receptor (PGR), and human epidermal growth factor receptor (ERBB2, also known as HER2), and the proliferation gene MKI67.

### PDX models

We included 21 PDX models of triple-negative breast cancer (TNBC) characterized previously at the Institut Curie (Table 1; refs. 25, 26). Transcriptome data were acquired using the Affymetrix Human Gene 1.1 ST Array applying standard procedures from the Institut Curie genomics platform. We use the tumor growth inhibition (TGI) value determined by the equation below as a measure of docetaxel response (25, 26). We classified PDX models as a high-responder having a TGI > 60% and a poor-responder having a TGI < 30%. RTV is relative tumor volume.

$$TGI(\%) = \left(1 - \frac{RTV_{treated}}{RTV_{control}}\right) \times 100$$

### Organoids derived from colorectal cancer patients

We included 15 organoids derived from colorectal cancer patients previously characterized by Clevers and colleagues (27). The Affymetrix gene expression data and drug response are publicly available (GEO accession: GSE64392). For the docetaxel response, we classified 7 organoids as poor-responders ( $IC_{50} \geq 0.362 \mu\text{mol/L}$ ) and 8 organoids as high-responders ( $IC_{50} \leq 0.151 \mu\text{mol/L}$ ); for Irinotecan, we classified 6 poor-responders ( $IC_{50} \geq 70.0 \mu\text{mol/L}$ ) and 9 high-responders ( $IC_{50} \leq 25 \mu\text{mol/L}$ ).

**Table 1.** Characteristics of the PDX models and the Institut Curie patient cohort

Characteristics	PDX models	
	High-responders	Poor-responders
Tumor type		
Primary		17
Metastatic		4
Docetaxel response		
High-responder (TGI > 60%)	8	
Poor-responder (TGI < 30%)		10
Adriamycin/cyclophosphamide response		
High-responder	6	
Poor-responder		13
	Institut Curie patient samples	
	High-responders	Poor-responders
Mean follow-up (years)	4.54 ± 1.21	5.81 ± 2.56
23 HER2 <sup>+</sup> patients	11	12
Clinical tumor stage		
T2	6 (55%)	1 (8%)
T3	4 (36%)	6 (50%)
T4	1 (9%)	5 (42%)
Clinical nodal status		
N0	4 (36%)	2 (17%)
N1	6 (55%)	4 (33%)
N2	1 (9%)	4 (33%)
N3	0 (0%)	2 (17%)

All PDXs are TNBC models. For more information on the PDX models, see references 25 and 26. For more information on the HER2<sup>+</sup> patients, see Materials and Methods.

### Analysis of gene expression data

For Affymetrix microarray datasets with multiple probe sets, we used collapseRows function from the WGCNA R package using the maxMean model to merge multiple probes into one. For NanoString nCounter analysis, total RNA (50 ng per sample) was assayed on a Gen2 nCounter platform at the Institut Curie Genomics Platform according to the manufacturer's instructions. We normalized the data following published (29) and NanoString guidelines (NanoString). Briefly, we first normalized using the geometric mean of the spiked-in positive controls (NanoString), we then subtracted background using the negative controls provided by NanoString, and finally we normalized by scaling with the geometric mean of the housekeeping genes ACTB, CLTC, and TUBB and used the  $\text{Log}_2$  values for all computational analyses.

### Random Forest classification

We exploited Random Forest classification using the randomForest R package (30) to identify gene panels whose expression pattern most accurately predict the TGI for the PDX models and the extent of response for the patients. We chose Random Forest classification based on four factors: (i) It takes into account the relationships between genes, offering an improved analytical technique over differential expression alone; (ii) It does not over fit the data, making it easier to train a classifier on one cohort and validate it on an independent cohort, thus generating general conclusions as to the importance of different genes in the classification; (iii) The method is fast and does not require parameter fitting; and (iv) It calculates the importance of each feature in the classification, simplifying the feature selection process (30, 31). Importantly, this method is particularly well suited for cases having small sample sizes with a large number of observations, such as patient cohorts with gene expression data (32). Moreover, Random Forests have been shown to be the most effective among nearly 200 classifiers recently tested in real-world problems (33). We built forests comprising 10,001 trees (an odd number ensures a deterministic model), and we kept all other settings at default. To identify the minimum effective gene panel, we ranked each gene's ability to classify samples using their Mean Decrease in Gini (MDG) applying a leave-one-out (LOO) approach and averaging the MDG across all permutations. We performed feature selection by sequentially adding genes in order of average MDG and calculated the internal out-of-bag (OOB) error rate across three repeats. For testing particular gene panels, we set the "mtry" variable to the number of genes in the panel, whereas for identifying important genes, we set mtry equal to the square root of the number of total genes. We defined the optimal panel as the one that gives the lowest OOB error averaged across Random Forest iterations. We assessed the performance of the panel by measuring the area under the receiver operating characteristic curve (AUC) using a LOO approach, measuring the probability of classification of the left-out sample. We clustered the samples based on their proximity matrix supplied by the Random Forest algorithm, which represents how similar two samples are based on how often they are assigned to the same terminal node.

### Random generalized linear model

We exploit random generalized linear model (RGLM) using the randomGLM R package (34). Briefly, RGLM is based on bootstrap aggregation of generalized linear models where the features (covariates) are selected using forward regression. For identifying

important genes, we used the default values for the parameters  $nBags$ ,  $nFeaturesInBag$ , and  $nCandidateCovariates$ . Following the same LOO approach as used for random forest, we analyzed the 21 TNBC PDX models using the TGI as a measure of docetaxel response (continuous response). For predictions using the distinct gene panels shown in Supplementary Fig. S2A, we set  $nCandidateCovariates = nFeaturesInBag$ .

### Institut Curie patient cohort

We chose a cohort of patients based on the fact that they received docetaxel as the single chemotherapy agent, they had available formalin-fixed paraffin-embedded tissue samples, and the corresponding clinical annotation was available. Twenty-three  $\text{HER2}^+$  patients diagnosed and treated at the Institut Curie were retrospectively reviewed. Each patient received docetaxel preoperatively (neoadjuvant setting) for at least 6 courses (in combination with trastuzumab). Clinical characteristics including treatment, follow-up time, response, clinical tumor and nodal stage, and histology are provided in Table 1 and Supplementary Table S1. The occurrence of a complete response (CR) was defined as the absence of residual invasive carcinoma in the breast and regional lymph nodes. Medical oncologists analyzed pathologic response according to the Chevallier and colleagues (35) and Sataloff and colleagues' (36) classifications and classified the patients into having a CR, major partial response ( $\text{PR}^{\text{maj}}$ ), partial response (PR), or stable disease (SD). For our binary analysis, we classified patients as high-responders if they achieved CR or a  $\text{PR}^{\text{maj}}$  and as poor-responders if they only achieved PR or SD at the time of surgical removal of the tumor. We applied the Freeman-Halton extension of the Fisher exact probability test for tumor stage and nodal stage. While the Fisher test is significant only for tumor stage ( $P < .04$ ), this may be due to the small patient sample size. Importantly, we applied a Wilcoxon Rank Sum test to the 18 genes in the panel and find that only 5 genes are significantly different between tumor stages T2 and T4 (*ACTL6A*,  $P = 0.001$ ; *BCL7C*,  $P = 0.035$ ; *HLTF*,  $P = 0.005$ ; *RUVBL1*,  $P = 0.022$ ; *STAG1*,  $P = 0.008$ ). However, clustering the gene expression for the 18 chromatin regulator panel according to tumor stage is not sufficient to distinguish the extent of patient response.

### NCI-60 database and pharmacogenomics analysis

The NCI-60 database, available using CellMiner or the NCI Developmental Therapeutics Program (DTP), contains previously normalized and filtered whole-exome sequencing, mRNA expression, promoter methylation, and drug activity, which are publicly available from CellMiner (<http://discover.nci.nih.gov/cellminer/>) or the NCI DTP (<http://dtp.cancer.gov>). Details regarding acquisition of drug activity data, promoter methylation, mRNA expression, and mutation profiles, together with their normalization and analysis, have been previously reported (37, 38). Briefly, we analyzed all chromatin regulator genes in the NCI-60 database to identify mutations, including homozygous deletions, heterozygous deletions, or not expressed. We analyzed the docetaxel response using the NSC-628503 classifier and paclitaxel response using the NSC-125973 classifier. Positive Z-scores represent sensitive and negative Z-scores represent resistant cell lines.

### Cells, antibodies, and viability studies

We purchased HAP1 knockout cell lines from Horizon Discovery in August 2015, and the knockouts were confirmed using

Western blot analysis. Cells were plated in triplicate at a density of 2,500 cells/well, and grown in complete IMDM glutamax media (Gibco) supplemented with 10% FBS and 1% penicillin and streptomycin, in 5% CO<sub>2</sub> at 37°C. We treated the cell lines with varying doses of docetaxel and paclitaxel. Cell viability was evaluated after 3, 4, and 8 days of treatment using CellTiter-Glo (Promega) luminescent assay on a Victor X5 plate reader (Perkin Elmer). We used commercial antibodies: SMARCA4 (Santa Cruz Biotechnology; sc-17796), SMARCA2 (Abcam; ab15597), ARID1B (Abcam; ab57461), gamma-tubulin (Sigma; T5326), ARID1A (Santa Cruz Biotechnology; sc-32761), ARID2 (Santa Cruz Biotechnology; sc-166117), PBRM1 (Bethyl; A-301-591A-M), and Lamin B1 (Abcam; ab16048). We used the Memcode Protein Stain Kit (Thermo Scientific) to detect transferred proteins to nitrocellulose membranes. We used secondary antibodies conjugated with horseradish peroxidase (Interchim) and revealed the signal by chemiluminescence substrate from Pierce (SuperSignal West Pico).

#### Ethics statement

According to French regulation, patients at the Institut Curie were informed of the types of experiments performed with the tumor specimens and did not express any opposition. The Breast Cancer Study Group and the Clinical Research Study Committee of the Institut Curie approved the study.

## Results

### A chromatin regulator gene panel distinguishes docetaxel high-responders and poor-responders in TNBC PDX models

We first analyzed 21 PDX models of TNBC (Table 1; refs. 25, 26) with available Affymetrix gene expression data and the corresponding TGI to docetaxel as a measure of response. Whereas most gene expression studies employ univariate measures of differential expression between high-responders and poor-responders (reviewed in ref. 39), we exploit Random Forest classification (refs. 30, 31; see Materials and Methods), a multivariate approach that is more sensitive to relationships between genes, to identify critical chromatin regulators whose expression pattern best predicts the TGI to docetaxel. From a list of 551 chromatin regulator genes (Supplementary Fig. S1), our strategy (Fig. 1) identified a panel of 19 chromatin regulators—*HDAC5*, *HDAC7*, *SMARCA4*, *SMARCA1*, *ARID2*, *HP1BP3*, *MED13*, *MLL2*, *MLL4*, *HIST1H2BM*, *EIF2C3*, *SOX5*, *SOX18*, *MBD4*, *MBD6*, *MCM4*, *RBBP4*, *RAD21*, and *BRDT*—that can predict the TGI with a strong correlation to the measured TGI ( $R^2 = 0.743$ ; Fig. 2A). To support this finding, we perform feature selection using a second approach, RGLM (34). Remarkably, though RGLM and Random Forest Classification rely on very different measures to determine variable importance (34, 40), we find that the top 5 important genes according to RGLM are also identified by Random Forest, with 9 common overall (*HDAC5*, *HDAC7*, *SMARCA4*, *SMARCA1*, *MED13*, *HIST1H2BM*, *SOX5*, *SOX18*, and *RBBP4*). When comparing both methods, we found a more robust predictive power for Random Forest (Supplementary Fig. S2A), which we chose along with its corresponding 19-chromatin regulator gene panel for further analysis.

We find that the 19-chromatin regulator gene panel readily distinguishes high-responders (TGI > 60%) and poor-responders (TGI < 30%; Fig. 2B) with an AUC of 0.925 (Fig. 2C). Moreover, the gene panel outperforms 100 random, 19-member

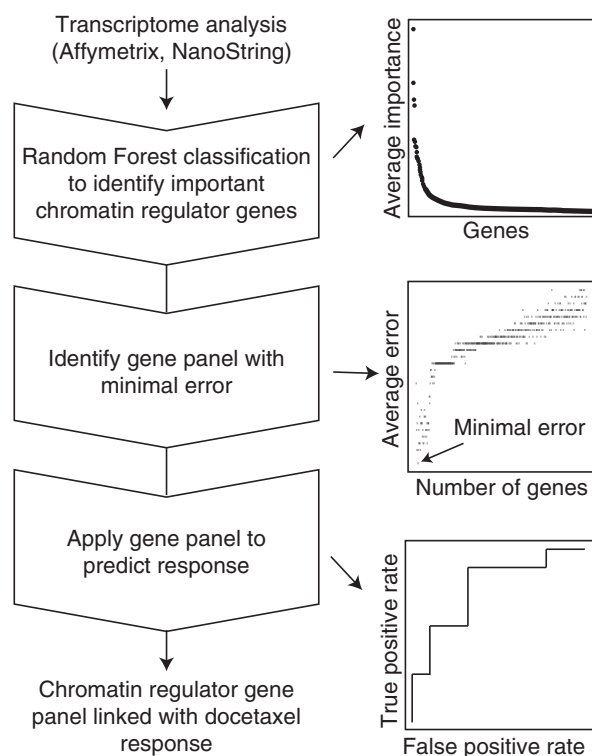


**Figure 1.**

A bioinformatics approach to identify gene panels predictive of response. Random Forest classification of gene expression data generated by Affymetrix microarrays or the Nanostring nCounter system provides a list of genes ordered by importance in distinguishing drug response. Starting with the most important gene, progressive gene panels are built, and the OOB error is calculated. The prediction accuracy of the gene panel having the minimal predictive error is then characterized using a proximity matrix and ROC curve.

chromatin regulator panels (Fig. 2D; Supplementary Fig. S2B), further validating the robustness of the method. Importantly, the chromatin regulator gene panel fails to segregate the PDX data according to their response to a combination of Adriamycin (doxorubicin), a topoisomerase II inhibitor, and cyclophosphamide (AUC = 0.397; Fig. 2E; Supplementary S2C). This suggests that the gene panel is selective for the response to docetaxel.

We next asked whether the ability of these chromatin regulators to classify docetaxel responders was valid in a cancer model for a different organ. We analyzed published Affymetrix gene expression data from organoids derived from colorectal cancer patients and the corresponding responses to treatment with either docetaxel or Irinotecan, a DNA topoisomerase I inhibitor (GEO accession: GSE64392; ref. 27). Only 10 of the 19 genes in the panel are available in this published dataset, yet the 10 genes exhibit the same selective trend for docetaxel (Supplementary Fig. S2D and S2E) as seen in the PDX models. Taken together, we find that a small panel of chromatin regulator genes allow the segregation of docetaxel high-responders and poor-responders.

### The NanoString nCounter system may provide higher resolution predictive information

The recent application of the NanoString nCounter system to the clinical setting (11) prompted us to test whether the ability of

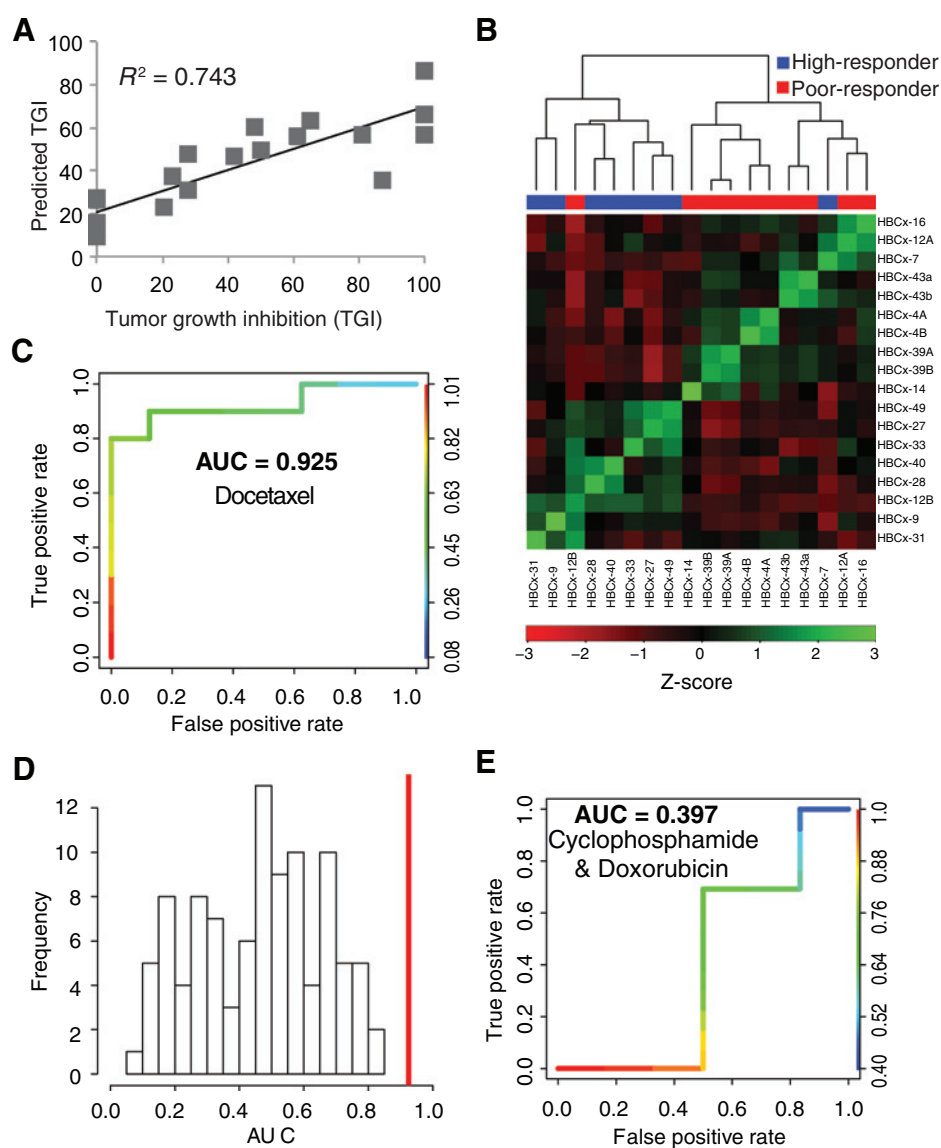


**Figure 2.** A chromatin regulator gene panel selectively distinguishes docetaxel high-responders and poor-responders. A, correlation of the TGI values predicted using the chromatin regulator gene panel to the measured TGI of the PDX models to docetaxel ( $R^2 = 0.743$ ). B, clustering of 18 PDX models according to the expression of the chromatin regulator gene panel and the response to docetaxel (high-responders: TGI > 60%; poor-responders: TGI < 30%). C, ROC curve for the chromatin regulator gene panel to classify the response of 18 PDX models to docetaxel. AUC = 0.925. Color indicates the cut-off threshold for classification. D, a histogram of AUC values for 100 random 19-member chromatin regulator gene panels to classify docetaxel response in the 18 PDX models. The red line represents the AUC for the chromatin regulator gene panel revealed using our approach. E, ROC curve for the chromatin regulator gene panel to classify the response of 19 PDX models to Adriamycin (doxorubicin) and cyclophosphamide (25, 26). AUC = 0.397. Color indicates the cut-off threshold for classification.

chromatin regulators to classify high-responders and poor-responders is validated using this approach. We isolated RNA from 9 of our previously characterized TNBC PDX models encompassing a range of TGI values and measured the gene expression of all chromatin regulators by NanoString (see Materials and Methods). We first compared the chromatin regulator gene expression data between Affymetrix and NanoString (Fig. 3A; Supplementary Fig. S3). We found that among the 19 chromatin regulators, 15 correlate well. We also found four outliers common across most samples (*SOX18*, *RBBP4*, *HIST1H2BM*, and *MED13*), for which the gene expression values are consistently higher when generated via Affymetrix. Notably, when applying the full 19-chromatin regulator gene panel to predict the TGI for the 9 PDX models, the NanoString values, though similar, outperform Affymetrix ( $R^2 = 0.77$  for NanoString;  $R^2 = 0.70$  for Affymetrix; Fig. 3B). These data reinforce the robustness of the method and results, and prompted us to further explore the quantitative NanoString technology to measure gene expression of chromatin regulators.

**A chromatin regulator gene panel distinguishes responders in HER2<sup>+</sup> breast cancer patients treated with docetaxel**

We next sought to generate NanoString expression data for the same 551 chromatin regulators (Supplementary Fig. S1) in a patient cohort treated with docetaxel. Cancer patients rarely receive single-agent chemotherapy regimens; however, we identified a cohort of 23 HER2<sup>+</sup> breast cancer patients treated at the Institut Curie who received docetaxel as the sole cytotoxic agent (Table 1; Supplementary Table S1), in combination with an anti-HER2 molecularly targeted therapy trastuzumab (Herceptin). We first classified the patients into four subgroups, those achieving CR, a PR<sup>maj</sup>, only a PR, or SD, at the time of surgical removal of the tumor. Random Forest classification identified a panel of 18 chromatin regulators—*HIST4H4*, *DNMT3A*, *HLTF*, *BCL7C*, *SENP5*, *MED29*, *SOX9*, *MTA3*, *MED11*, *MED7*, *KDM7A*, *ACTL6A*, *RUVBL1*, *ARID3A*, *STAG1*, *HDAC3*, *BPTF*, and *UBN1*—that robustly distinguish the four subgroups (Fig. 4A). Indeed, the 18-chromatin regulator gene panel accurately classifies 6 of 7 CR

Downloaded from <http://aacrjournals.org/mct/article-pdf/15/7/1772/1552378/1768.pdf> by guest on 18 May 2022

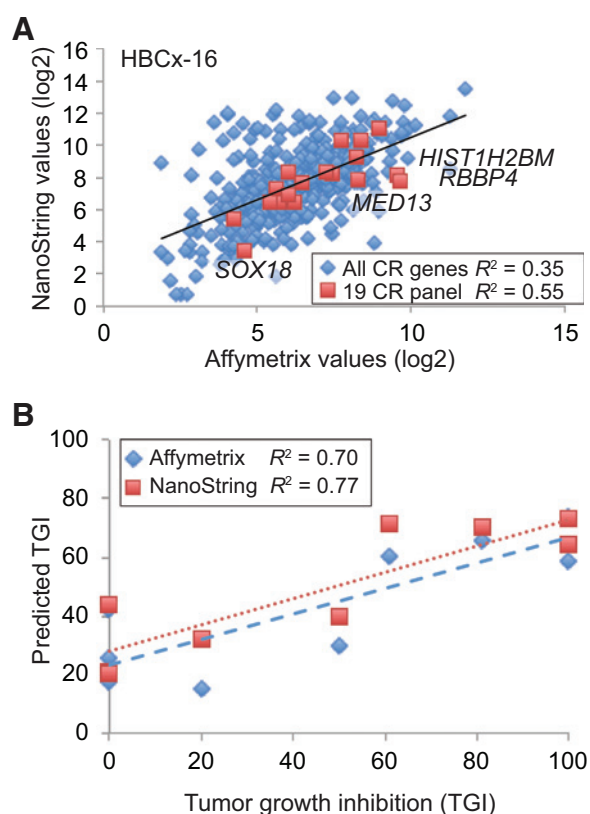


**Figure 3.** Comparison of gene expression values generated by Affymetrix and NanoString. A, gene expression values for all chromatin regulators (blue) and the 19-chromatin regulator gene panel (red) measured in one PDX model (HBCx-16). The four outliers are labeled. B, correlation of the TGI values predicted using the limited chromatin regulator gene panel to the measured TGI of 9 PDX models to docetaxel using expression values generated by Affymetrix (blue,  $R^2 = 0.70$ ) and NanoString (red,  $R^2 = 0.77$ ). CR, chromatin regulators.

(86%), 3 of 4 PR<sup>maj</sup> (75%), 9 of 9 PR (100%), and 1 of 3 SD (33%), for a total accuracy of 83% (Fig. 4B). To further analyze this chromatin regulator gene panel, we separated the patients into "high-responders" (CR and PR<sup>maj</sup>) and "poor-responders" (PR and SD), and confirmed that data normalization (see Materials and Methods) does not bias the two groups (Supplementary Fig. S4A), and that each subgroup has similar proliferation levels determined by the RNA expression of *MKI67* (Supplementary Fig. S4B). Furthermore, we confirmed that hormone status alone (HR; sum of *ESR1* and *PGR*; Supplementary Fig. S4C) and tumor stage (Supplementary Fig. S4D) are not sufficient to predict response. We find that the chromatin regulator gene panel robustly distinguishes the high-responders and poor-responders (AUC = 0.833; Fig. 4C) and outperforms 100 random, 18-member CR gene panels (Supplementary Fig. S4E and S4F). Importantly, when we build the classification model on the 23 patients as a training set, and apply it to 4 patients whose expression was measured in a distinct NanoString experiment, the gene panel accurately classifies all 4 patients (100%). These data further highlight the potential clinical value of chromatin regulators to predict a range of responses to docetaxel, and stress a need to include chromatin regulators in the clinical setting and investigate

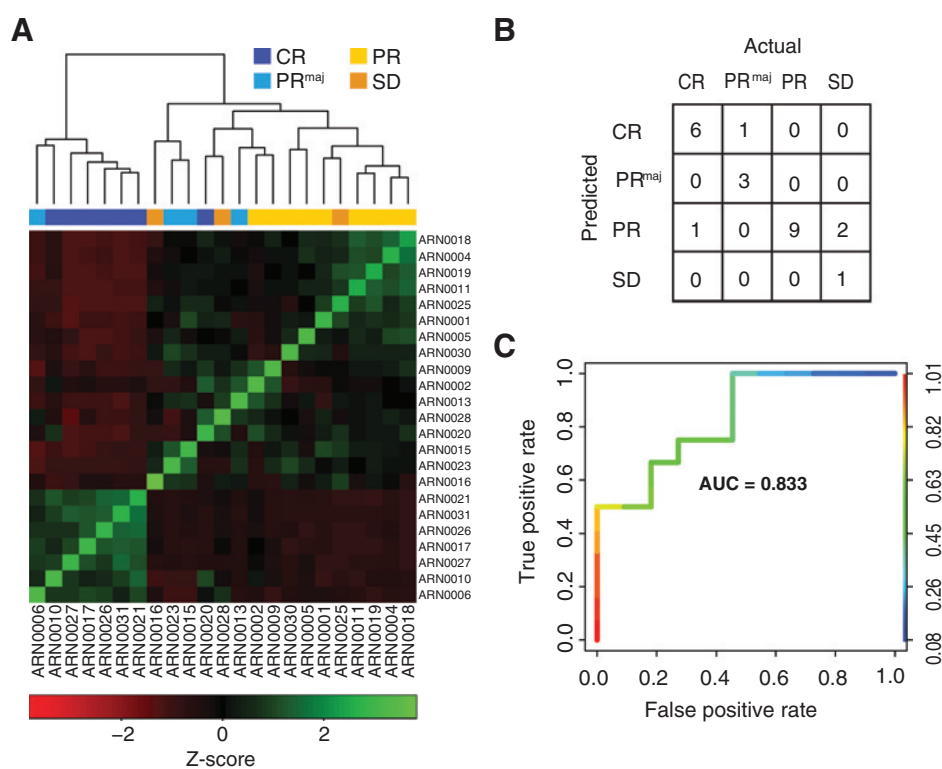
their application as biomarkers of patient response in larger cohorts and for other drugs.

### The SWI/SNF remodeler complex is associated with the docetaxel response

Key SWI/SNF chromatin remodeler components are common features to the two chromatin regulator gene panels that were derived from different cancer types (*SMARCA4*, *SMARCAL1*, *ARID2* in the TNBC PDX; *HLTF*, *BCL7C*, *ACTL6A* in the HER2<sup>+</sup> patients), suggesting a common pathway. We then analyzed the two panels using the STRING tool (41), a database of known and predicted protein-protein interactions. We determine that many proteins participate in a large interaction network and that the SWI/SNF component *SMARCA4* is a key node (Fig. 5A). We thus further explored the link between SWI/SNF gene expression and the docetaxel response in a cellular context first using the comprehensive NCI-60 database. We find that the SWI/SNF chromatin remodeler is the most altered chromatin regulator in the NCI-60 database, of which *SMARCA4* and *HLTF* are the most altered components. These loss-of-function alterations include heterozygous or homozygous deletion or, in the case of *HLTF*, possible epigenetic silencing through promoter methylation (Supplementary Fig. S5A; ref. 42). Notably, of the 14 NCI-60 cell lines from breast, colorectal, leukemia, lung, ovarian, and renal cancers featuring a loss of function of *SMARCA4*, *HLTF*, or of the third most altered SWI/SNF component *ARID1A*, 13 (93%) are sensitive to docetaxel (Fig. 5B). This recapitulates the trend observed in the PDX models, where gene expression of the SWI/SNF components inversely correlates with docetaxel sensitivity. We then asked whether downregulating SWI/SNF using pharmacologic and genetic approaches could affect docetaxel sensitivity by targeting *SMARCA4*, the node in the interaction network. For this, we first treated HAP1 cells with a combination of docetaxel and PFI-3, a recently described bromodomain inhibitor selective for *SMARCA2/4* (43); however, this combination did not further alter docetaxel sensitivity in the tested conditions (Supplementary Fig. S5B). This suggests that targeting the *SMARCA4* bromodomain is not sufficient to disrupt the functional node. We therefore decided to exploit genetic interference. We treated the HAP1 cell lines wildtype for SWI/SNF (HAP1-WT) and knockout for *SMARCA4* (*SMARCA4*-KO) and *SMARCA2* (*SMARCA2*-KO), a SWI/SNF component not appearing in our gene panels (Supplementary Fig. S5C), with docetaxel and assessed cell viability. We observe a 4-fold decrease in the IC<sub>50</sub> for docetaxel in the *SMARCA4*-KO cell line relative to wildtype (Fig. 5C), consistent with the expression pattern in the PDX. Taken together, our results show a functional association between the SWI/SNF chromatin remodeler and the docetaxel response in the NCI-60 database and in the HAP1 cell line. These data warrant further exploration of pharmacologic intervention to exploit this actionable type of target in combination with docetaxel to increase sensitivity and potentially combat inherent and acquired resistance.

### Discussion

Chromatin regulators have proven to be powerful clinical tools, most notably as therapeutic targets (e.g., histone deacetylase and DNA methyltransferase inhibitors), although increasing evidence also points to their prognostic value. Indeed, our earlier work identified the mid subunit (p60) of the histone chaperone

**Figure 4.**

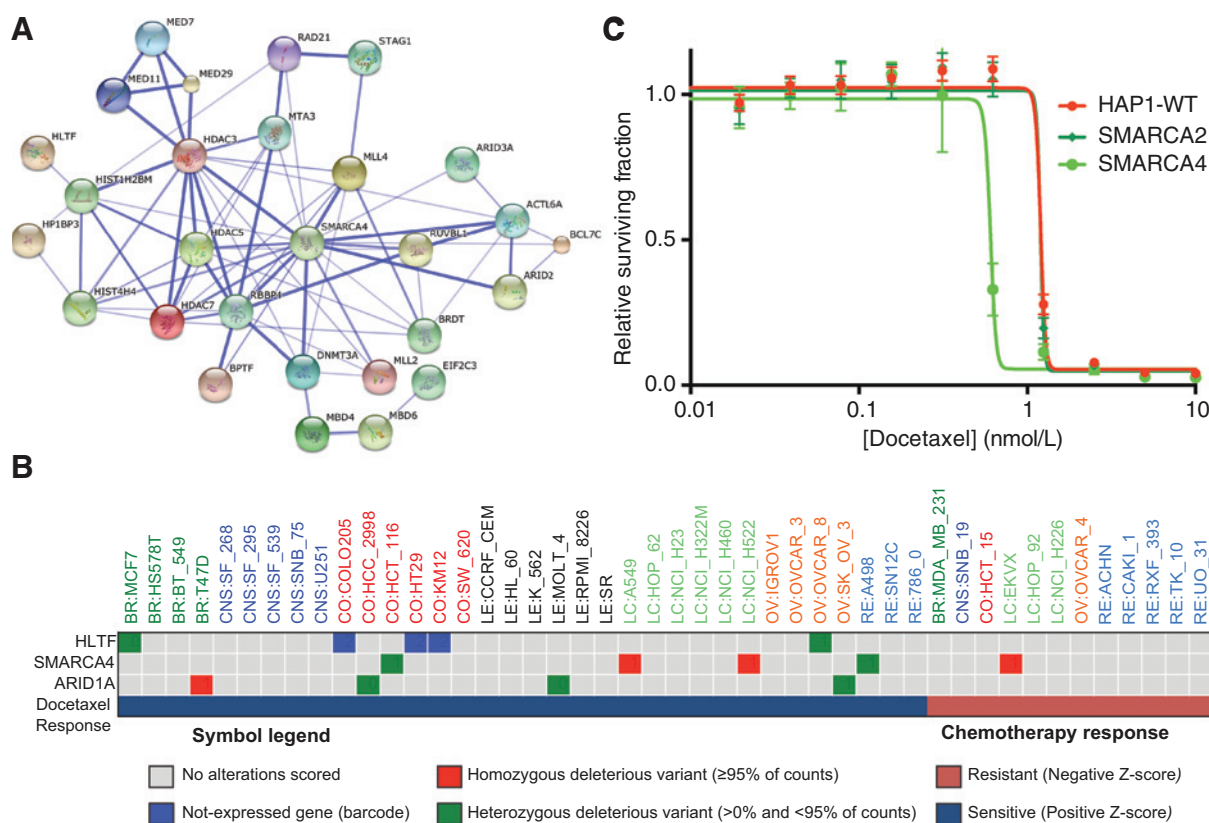
A chromatin regulator gene panel can distinguish response in HER2<sup>+</sup> patients treated with docetaxel. A, clustering of a cohort of 23 HER2<sup>+</sup> patients diagnosed and treated at the Institut Curie according to the expression of an 18-chromatin regulator gene panel measured using the NanoString nCounter system and the patient response determined at the time of surgical removal of the tumor. B, performance of the chromatin regulator gene panel to classify the patients into the four subgroups. C, ROC curve for the chromatin regulator gene panel to classify the patients as either a high-responder (CR and PR<sup>maj</sup>) or poor-responder (PR and SD). AUC = 0.833. Color indicates the cut-off threshold for classification.

chromatin assembly factor 1 complex (CAF-1) as well as heterochromatin protein 1 alpha (HP1 $\alpha$ ) as cancer proliferation markers (44, 45). Furthermore, the histone chaperone ASF1B has prognostic value for metastasis in breast cancer and is upregulated in several tumors (46, 47). While the expression of certain chromatin regulators correlates with proliferation (refs. 44, 45, 47; Supplementary Fig. S3C and S3D), the potential clinical value extends beyond markers of proliferation. Indeed, we recently showed that the dedicated CenH3 histone chaperone HJURP (Holliday Junction Recognizing Protein) outperforms Ki67 as a prognostic marker to distinguish good and poor prognosis luminal A breast carcinomas to help rule out unnecessary chemotherapy (48). In addition, several studies demonstrate that changes to the dosage of chromatin regulators, through altered expression or pharmacologic inhibition, alter chemotherapy efficacy (7, 16, 18). This opens avenues for exploiting chromatin regulators in diagnostics and in combination therapy to improve clinical response. Our study extends the clinical value of chromatin regulators by demonstrating their ability to distinguish docetaxel high-responders and poor-responders in PDX models of TNBC (Fig. 2) and HER2<sup>+</sup> patients (Fig. 4). Importantly, the ability to distinguish docetaxel responders is observed in both PDX TNBC models and organoids derived from colorectal cancer patients (Supplementary Fig. S2D and S2E). This suggests a mechanistic link between these distinct chromatin regulators and the docetaxel response. Our data from the NCI-60 dataset further suggest a potential broad clinical applicability.

To determine how to best translate chromatin regulator gene panels into valuable clinical tools, we compared the methods used to generate gene expression data: Affymetrix microarrays, which rely on an enzymatic amplification step, and the count-based, quantitative NanoString technology. Gene expression

values for all chromatin regulators largely correlate between the two techniques, with some reproducible differences (Fig. 3A; Supplementary Fig. S3). Importantly, NanoString outperforms Affymetrix in predicting the TGI of the PDX models tested (Fig. 3B). Notably, NanoString, the assay of choice for the PAM50 prognostic signature, has a probeset capacity of 800 genes. Therefore, it would be interesting to supplement the PAM50 prognostic signature in the clinical research setting with chromatin regulators to help develop a diagnostic tool that will inform about chemotherapy choices. Indeed, the results presented here support the analysis of chromatin regulator genes in larger cohorts, including other breast cancer subtypes, and could extend to other cancers. In our study, we focus on expression at the RNA level; however, future work should also assess the protein level of these chromatin regulators. Interestingly, NanoString technology enables simultaneous quantification of DNA, RNA, and protein levels in the same sample. Integrating the genomic, transcriptomic, and proteomic aspects in a quantitative manner could provide a more complete diagnostic assessment.

The chromatin remodeler SWI/SNF has been implicated in maintaining genome stability and preventing tumorigenesis (reviewed in ref. 49), and it is the most altered chromatin regulator in solid tumors (based on TCGA, ICGC, and literature; refs. 50, 51). SMARCA4 and HLTf, two SWI/SNF components that appear in our gene panels, are the most altered SWI/SNF components in the NCI-60. Consistent with our hypothesis, they regulate chromatin structures that are critical for chromosome segregation, the biologic target for docetaxel. HLTf has an important role in the G<sub>2</sub>-M transition, regulating the availability of transcripts for key factors involved in chromosome cohesion and condensation (52). Given the biologic consequences of dosage imbalances in

**Figure 5.**

The SWI/SNF chromatin remodeler is associated with the docetaxel response. A, protein interaction network of chromatin regulators appearing in the PDX panel and patient panel predicted using STRING (41) with a confidence cut-off of 0.4. Line-weight represents confidence in predicted interactions. B, cell lines from the NCI-60 database with a reported docetaxel (NSC-628503) response are included. Alterations of SWI/SNF genes are represented by colored squares. The columns are organized first by docetaxel sensitivity and then by tissue of origin (color-coded) where BR, breast; CNS, central nervous system; CO, colorectal; LE, leukemia; LC, lung; OV, ovarian; RE, renal. The rows present the SWI/SNF genes ranked by alteration frequency in the NCI-60. C, the viability of HAP1 wild-type (WT) cells and knockout cells for SMARCA4 (SMARCA4-KO) and SMARCA2 (SMARCA2-KO) after 8 days of varying concentrations of docetaxel. The fraction of viable cells is plotted versus the docetaxel concentration.

chromatin regulators (7), changes to the stoichiometry of select SWI/SNF components—or other chromatin regulators that participate in the interaction network (Fig. 5A)—could contribute to aberrant chromatin structures and a perturbed chromatin landscape that alters drug response. SMARCA4 and SMARCA2 are ATPases essential for SWI/SNF function, but they are not functionally equivalent. As one example, depletion of SMARCA4, but not SMARCA2, in primary mouse fibroblasts disrupts pericentric heterochromatin (53), a chromatin domain that participates in cross-talk with centromeric chromatin (54). This nonredundancy is consistent with our observation that the HAP1 model cell line lacking SMARCA4, but not SMARCA2, has an increased sensitivity to docetaxel (Fig. 5C).

Our data strongly suggest that SWI/SNF is a promising candidate biomarker to identify docetaxel-sensitive patients. It also identifies SWI/SNF as an actionable therapeutic target to increase docetaxel efficacy and combat inherent and acquired resistance. Here, we find that combining docetaxel with PFI-3, a SMARCA2/4 bromodomain inhibitor (43), does not increase docetaxel sensitivity in our model cell line. This suggests that other modes of interference in their function are likely necessary, and future work should consider whether targeting the ATPase catalytic domain

could represent a more relevant therapeutic target, as previously suggested (43). In addition, other avenues could be explored by acting on other SWI/SNF components, other proteins in the interaction network, or posttranslational modifications that regulate protein function. Interestingly, the SMARCA4-KO cell line has a decreased expression of several SWI/SNF components (Supplementary Fig. S5D). This supports the role of SMARCA4 as a key node and suggests that targeting the complex may be more clinically relevant. In addition to docetaxel, other drug combinations could also be envisaged (Supplementary Fig. S5D and S5E; refs. 55, 56), and this may be particularly critical to deal with a heterogeneous disease. Further investigation of how SWI/SNF dosage imbalances alter its function and the chromatin landscape, potentially through single-cell approaches, could help delineate how to best translate SWI/SNF alterations into therapeutic advantages, including identifying patient populations with a heightened sensitivity to docetaxel and to combat docetaxel resistance. Finally, given that both metabolic changes and immune responses relate to chromatin-based events (57, 58), the role of the tumor microenvironment and how it could affect chromatin regulator behavior and the subsequent drug response will also be interesting to explore.

## Conclusion

We demonstrate that the expression of a panel of chromatin regulator genes correlates with the docetaxel response in several systems, and we identify a new way to combat docetaxel resistance by targeting the SWI/SNF chromatin remodeler. Our data highlight the necessity to validate the clinical value of distinct chromatin regulators in larger cohorts to identify docetaxel-sensitive patients and their applicability to other drugs. Importantly, our strategy may prove useful in deriving companion diagnostics, including for drugs still in development, and to identify novel chromatin targets for combination therapy with other drugs, including chemotherapies, metabolic drugs, and immunotherapies.

## Disclosure of Potential Conflicts of Interest

No potential conflicts of interest were disclosed.

## Authors' Contributions

**Conception and design:** Z.A. Gurard-Levin, V. Pancaldi, P. Cottu, G. Almouzni  
**Development of methodology:** Z.A. Gurard-Levin, L.O.W. Wilson, V. Pancaldi, E. Marangoni, Y. Pommier, G. Almouzni

**Acquisition of data (provided animals, acquired and managed patients, provided facilities, etc.):** Z.A. Gurard-Levin, S. Postel-Vinay, C. Reyes, E. Marangoni, D. Gentien, Y. Pommier, P. Cottu

**Analysis and interpretation of data (e.g., statistical analysis, biostatistics, computational analysis):** Z.A. Gurard-Levin, L.O.W. Wilson, V. Pancaldi, F.G. Sousa, A. Valencia, Y. Pommier, P. Cottu, G. Almouzni

**Writing, review, and/or revision of the manuscript:** Z.A. Gurard-Levin, L.O.W. Wilson, S. Postel-Vinay, F.G. Sousa, E. Marangoni, D. Gentien, P. Cottu, G. Almouzni

## References

- Filipescu D, Muller S, Almouzni G. Histone H3 variants and their chaperones during development and disease: Contributing to epigenetic control. *Annu Rev Cell Dev Biol* 2014;30:615–46.
- Gurard-Levin ZA, Quivy JP, Almouzni G. Histone chaperones: Assisting histone traffic and nucleosome dynamics. *Annu Rev Biochem* 2014;83:487–517.
- Skulte KA, Phan L, Clark SJ, Taberlay PC. Chromatin remodeler mutations in human cancers: Epigenetic implications. *Epigenomics* 2014;6:397–414.
- Sullivan LL, Boivin CD, Mravinac B, Song IY, Sullivan BA. Genomic size of CENP-A domain is proportional to total alpha satellite array size at human centromeres and expands in cancer cells. *Chromosome Res* 2011;19:457–70.
- Cleveland DW, Mao Y, Sullivan KF. Centromeres and kinetochores: From epigenetics to mitotic checkpoint signaling. *Cell* 2003;112:407–21.
- Baylin SB, Jones PA. A decade of exploring the cancer epigenome - biological and translational implications. *Nat Rev Cancer* 2011;11:726–34.
- Lacoste N, Woolfe A, Tachiwana H, Gareu AV, Barth T, Cantaloube S, et al. Mislocalization of the centromeric histone variant CenH3/CENP-A in human cells depends on the chaperone DAXX. *Mol Cell* 2014;53:631–44.
- Sorlie T, Tibshirani R, Parker J, Hastie T, Marron JS, Nobel A, et al. Repeated observation of breast tumor subtypes in independent gene expression data sets. *Proc Natl Acad Sci U S A* 2003;100:8418–23.
- Chia SK, Bramwell VH, Tu D, Shepherd LE, Jiang S, Vickery T, et al. A 50-gene intrinsic subtype classifier for prognosis and prediction of benefit from adjuvant tamoxifen. *Clin Cancer Res* 2012;18:4465–72.
- Paik S, Shak S, Tang C, Kim C, Baker J, Cronin M, et al. A multigene assay to predict recurrence of tamoxifen-treated, node-negative breast cancer. *N Engl J Med* 2004;351:2817–26.
- Wallden B, Storhoff J, Nielsen T, Dowidar N, Schaper C, Ferree S, et al. Development and verification of the PAM50-based Prosigna breast cancer gene signature assay. *BMC Med Genomics* 2015;8:54.
- Gyorffy B, Hatzis C, Sanft T, Hofstatter E, Aktas B, Pusztai L. Multigene prognostic tests in breast cancer: Past, present, future. *Breast Cancer Res* 2015;17:11.
- Patani N, Martin LA, Dowsett M. Biomarkers for the clinical management of breast cancer: International perspective. *Int J Cancer* 2013;133:1–13.
- Reis-Filho JS, Pusztai L. Gene expression profiling in breast cancer: Classification, prognostication, and prediction. *Lancet* 2011;378:1812–23.
- Alizadeh AA, Aranda V, Bardelli A, Blanpain C, Bock C, Borowski C, et al. Toward understanding and exploiting tumor heterogeneity. *Nat Med* 2015;21:846–53.
- Banelli B, Carra E, Barbieri F, Wurth R, Parodi F, Pattarozzi A, et al. The histone demethylase KDM5A is a key factor for the resistance to temozolomide in glioblastoma. *Cell Cycle* 2015;14:3418–29.
- Husain A, Begum NA, Taniguchi T, Taniguchi H, Kobayashi M, Honjo T. Chromatin remodeler SMARCA4 recruits topoisomerase 1 and suppresses transcription-associated genomic instability. *Nat Commun* 2016;7:10549.
- Sharma SV, Lee DY, Li B, Quinlan MP, Takahashi F, Maheswaran S, et al. A chromatin-mediated reversible drug-tolerant state in cancer cell subpopulations. *Cell* 2010;141:69–80.
- Wijdeven RH, Pang B, van der Zanden SY, Qiao X, Blomen V, Hoogstraat M, et al. Genome-wide identification and characterization of novel factors conferring resistance to topoisomerase II poisons in cancer. *Cancer Res* 2015;75:4176–87.
- Ringel I, Horwitz SB. Studies with RP 56976 (taxotere): A semisynthetic analogue of taxol. *J Natl Cancer Inst* 1991;83:288–91.
- Bonneau C, Gurard-Levin ZA, Andre F, Pusztai L, Rouzier R. Predictive and prognostic value of the TauProtein in breast cancer. *Anticancer Res* 2015;35:5179–84.
- Weigelt B, Pusztai L, Ashworth A, Reis-Filho JS. Challenges translating breast cancer gene signatures into the clinic. *Nat Rev Clin Oncol* 2012;9:58–64.

**Administrative, technical, or material support (i.e., reporting or organizing data, constructing databases):** Z.A. Gurard-Levin, C. Reyes, D. Gentien, G. Almouzni

**Study supervision:** Z.A. Gurard-Levin, G. Almouzni

## Acknowledgments

The authors thank Sergio Roman-Roman, Nicolas Dorvault (U981 INSERM), Christopher Mueller, Jean Gautier, and Bruno Amati (Mayent-Rothschild Sabbatical Scientists at Institut Curie) for critical comments on the article and the Almouzni lab for insightful discussions. They apologize to their colleagues whose work could not be cited due to space constraints.

## Grant Support

G. Almouzni's team is supported by la Ligue Nationale contre le Cancer (Equipe labellisée Ligue), the European Commission Network of Excellence EpiGeneSys [HEALTH-F4-2010-257082; an EpiGeneSys small call award to Z.A. Gurard-Levin and V. Pancaldi (2014)] ERC Advanced Grant 2009-AdG\_20090506 "Eccentric," ERC Proof of Concept N° 678563 "EPOCH28" to G. Almouzni, the European Commission large-scale integrating project FP7\_HEALTH-2010-259743 "MODHEP," ANR-11-LABX-0044\_DEEP and ANR-10-IDEX-0001-02 PSL, ANR "CHAPINHIB" ANR-12-BSV5-0022-02, ANR "Epicure" ANR-14-CE16-0009, ANR "CELLECTCHIP" ANR-14-CE10-0013, and Aviesan-ITMO cancer project "Epigenomics of breast cancer." Acquisition of the Nanostring platform was initiated and supported by ANR-10-IDEX-0001-02 PSL, ANR-11-LBX-0044, and Grant « INCa-DGOS- 4654 » SIRIC11-002. V. Pancaldi is supported by a FEBS fellowship. Y. Pommier and F.G. Sousa were supported by the NIH Intramural Program, Center for Cancer Research (Z01 BC 006150).

Received December 24, 2015; revised April 7, 2016; accepted April 26, 2016; published OnlineFirst May 16, 2016.

23. Wu MY, Fu J, Xiao X, Wu J, Wu RC. MiR-34a regulates therapy resistance by targeting HDAC1 and HDAC7 in breast cancer. *Cancer Lett* 2014;354:311–9.
24. Giovinazzi S, Lindsay CR, Morozov VM, Escobar-Cabrera E, Summers MK, Han HS, et al. Regulation of mitosis and taxane response by Daxx and Rassf1. *Oncogene* 2012;31:13–26.
25. Marangoni E, Vincent-Salomon A, Auger N, Degeorges A, Assayag F, de Cremoux P, et al. A new model of patient tumor-derived breast cancer xenografts for preclinical assays. *Clin Cancer Res* 2007;13:3989–98.
26. Romanelli A, Clark A, Assayag F, Chateau-Joubert S, Poupon MF, Servedy JL, et al. Inhibiting aurora kinases reduces tumor growth and suppresses tumor recurrence after chemotherapy in patient-derived triple-negative breast cancer xenografts. *Mol Cancer Ther* 2012;11:2693–703.
27. van de Wetering M, Francies HE, Francis JM, Bounova G, Iorio F, Pronk A, et al. Prospective derivation of a living organoid biobank of colorectal cancer patients. *Cell* 2015;161:933–45.
28. Geiss GK, Bumgarner RE, Birditt B, Dahl T, Dowidar N, Dunaway DL, et al. Direct multiplexed measurement of gene expression with color-coded probe pairs. *Nat Biotechnol* 2008;26:317–25.
29. Brumbaugh CD, Kim HJ, Giovacchini M, Pourmand N. NanoStriDE: normalization and differential expression analysis of NanoString nCounter data. *BMC Bioinformatics* 2011;12:479.
30. Breiman L. *Random Forests*. *Mach Learn* 2001;45:5–32.
31. Riddick G, Song H, Ahn S, Walling J, Borges-Rivera D, Zhang W, et al. Predicting in vitro drug sensitivity using Random Forests. *Bioinformatics* 2011;27:220–4.
32. Diaz-Uriarte R, Alvarez de Andres S. Gene selection and classification of microarray data using Random Forest. *BMC Bioinformatics* 2006;7:3.
33. Fernandez-Delgado M, Cernadas E, Barro S, Amorim D. Do we need hundreds of classifiers to solve real world classification problems? *J Mach Learn Res* 2014;15:3133–81.
34. Song L, Langfelder P, Horvath S. Random generalized linear model: A highly accurate and interpretable ensemble predictor. *BMC Bioinformatics* 2013;14:5.
35. Chevallier B, Roche H, Olivier JP, Chollet P, Hurlteloup P. Inflammatory breast cancer. Pilot study of intensive induction chemotherapy (FEC-HD) results in a high histologic response rate. *Am J Clin Oncol* 1993;16:223–8.
36. Sataloff DM, Mason BA, Prestipino AJ, Seinige UL, Lieber CP, Baloch Z. Pathologic response to induction chemotherapy in locally advanced carcinoma of the breast: A determinant of outcome. *J Am Coll Surg* 1995;180:297–306.
37. Reinhold WC, Sunshine M, Liu H, Varma S, Kohn KW, Morris J, et al. CellMiner: A web-based suite of genomic and pharmacologic tools to explore transcript and drug patterns in the NCI-60 cell line set. *Cancer Res* 2012;72:3499–511.
38. Sousa FG, Matuo R, Tang SW, Rajapakse VN, Luna A, Sander C, et al. Alterations of DNA repair genes in the NCI-60 cell lines and their predictive value for anticancer drug activity. *DNA Repair (Amst)* 2015;28:107–15.
39. Marchionni L, Wilson RF, Wolff AC, Marinopoulos S, Parmigiani G, Bass EB, et al. Systematic review: Gene expression profiling assays in early-stage breast cancer. *Ann Intern Med* 2008;148:358–69.
40. Saey Y, Inza I, Larranaga P. A review of feature selection techniques in bioinformatics. *Bioinformatics* 2007;23:2507–17.
41. Szklarczyk D, Franceschini A, Wyder S, Forslund K, Heller D, Huerta-Cepas J, et al. STRING v10: Protein-protein interaction networks, integrated over the tree of life. *Nucleic Acids Res* 2015;43:D447–52.
42. Moinova HR, Chen WD, Shen L, Smiraglia D, Olechnowicz J, Ravi L, et al. HlTF gene silencing in human colon cancer. *Proc Natl Acad Sci U S A* 2002;99:4562–7.
43. Vangamudi B, Paul TA, Shah PK, Kost-Alimova M, Nottebaum L, Shi X, et al. The SMARCA2/4 ATPase domain surpasses the bromodomain as a drug target in SWI/SNF-mutant cancers: Insights from cDNA rescue and PFI-3 inhibitor studies. *Cancer Res* 2015;75:3865–78.
44. De Koning L, Savignoni A, Boumendil C, Rehman H, Asselain B, Sastre-Garau X, et al. Heterochromatin protein 1alpha: A hallmark of cell proliferation relevant to clinical oncology. *EMBO Mol Med* 2009;1:178–91.
45. Polo SE, Theocharis SE, Klijanienko J, Savignoni A, Asselain B, Vielh P, et al. Chromatin assembly factor-1, a marker of clinical value to distinguish quiescent from proliferating cells. *Cancer Res* 2004;64:2371–81.
46. Abascal F, Corpet A, Gurard-Levin ZA, Juan D, Ochsenbein F, Rico D, et al. Subfunctionalization via adaptive evolution influenced by genomic context: The case of histone chaperones ASF1a and ASF1b. *Mol Biol Evol* 2013;30:1853–66.
47. Corpet A, De Koning L, Toedling J, Savignoni A, Berger F, Lemaitre C, et al. ASF1b, the necessary ASF1 isoform for proliferation, is predictive of outcome in breast cancer. *EMBO J* 2011;30:480–93.
48. Montes de Oca R, Gurard-Levin ZA, Berger F, Rehman H, Martel E, Corpet A, et al. The histone chaperone HJURP is a new independent prognostic marker for luminal A breast carcinoma. *Mol Oncol* 2015;9:657–74.
49. Brownlee PM, Meisenberg C, Downs JA. The SWI/SNF chromatin remodeling complex: Its role in maintaining genome stability and preventing tumorigenesis. *DNA Repair (Amst)* 2015;32:127–33.
50. Masliah-Planchon J, Bieche I, Guinebretiere JM, Bourdeaut F, Delattre O. SWI/SNF chromatin remodeling and human malignancies. *Annu Rev Pathol* 2015;10:145–71.
51. Shah MA, Denton EL, Arrowsmith CH, Lupien M, Schapira M. A global assessment of cancer genomic alterations in epigenetic mechanisms. *Epigenetics Chromatin* 2014;7:29.
52. Helmer RA, Martinez-Zaguilan R, Dertien JS, Fulford C, Foreman O, Peiris V, et al. Helicase-like transcription factor (HlTF) regulates G2/M transition, Wt1/Gata4/Hif-1a cardiac transcription networks, and collagen biogenesis. *PLoS One* 2013;8:e80461.
53. Bourgo RJ, Siddiqui H, Fox S, Solomon D, Sansam CG, Yaniv M, et al. SWI/SNF deficiency results in aberrant chromatin organization, mitotic failure, and diminished proliferative capacity. *Mol Biol Cell* 2009;20:3192–9.
54. Boyarchuk E, Filipescu D, Vassias I, Cantaloube S, Almouzni G. The histone variant composition of centromeres is controlled by the pericentric heterochromatin state during the cell cycle. *J Cell Sci* 2014;127:3347–59.
55. Bitler BC, Aird KM, Garipov A, Li H, Amatangelo M, Kossakov AV, et al. Synthetic lethality by targeting EZH2 methyltransferase activity in ARID1A-mutated cancers. *Nat Med* 2015;21:231–8.
56. Kim KH, Kim W, Howard TP, Vazquez F, Tsherniak A, Wu JN, et al. SWI/SNF-mutant cancers depend on catalytic and non-catalytic activity of EZH2. *Nat Med* 2015;21:1491–6.
57. Allan RS, Zueva E, Cammas F, Schreiber HA, Masson V, Belz GT, et al. An epigenetic silencing pathway controlling T helper 2 cell lineage commitment. *Nature* 2012;487:249–53.
58. Venneti S, Thompson CB. Metabolic modulation of epigenetics in gliomas. *Brain Pathol* 2013;23:217–21.